Tellus (2006), 58B, 31–40
Printed in Singapore. All rights reserved

TELLUS

Integrated studies of a photochemical smog episode in Hong Kong and regional transport in the Pearl River Delta of China

By T. J. WANG[1,2,*], K. S. LAM[2], M. XIE[1], X. M. WANG[3], G. CARMICHAEL[4] and Y. S. Li[2]
[1]*Department of Atmospheric Science, Nanjing University, Nanjing 210093, China;* [2]*Department of Civil and Structural Engineering, the Hong Kong Polytechnic University, Hong Kong, China;* [3]*Department of Environmental Science, Zhongshan University, China;* [4]*Center for Global and Regional Environmental Research, University of Iowa, USA*

(Manuscript received 17 February 2005; in final form 19 September 2005)

ABSTRACT

Air pollution in Hong Kong has close relations to synoptic systems, especially continental high pressure in cold season and tropical storms in the warm season. Here, a case study was performed of the characteristics of a photochemical pollution episode during March 27–31, 2000, in which the maximum concentrations of ozone (O_3), nitrogen oxides (NO_x), carbon monoxide (CO), respirable suspended particulates (RSP) and sulphur dioxide (SO_2) reached 265 μgm^{-3}, 2166 μgm^{-3} (roadside), 5405 μgm^{-3}, 349.3 μgm^{-3} and 221 μgm^{-3}, respectively. The O_3/CO and O_3/NO_x ratios were found to be 0.1 and 6.29, respectively, at rural site without significant correlation. At an urban site, moderate negative correlation was observed for O_3, CO, NO_x, where the ratios of O_3/CO and O_3/NO_x were relatively lower (0.03 and 0.21, respectively). The episode lasted 2 d in the Hong Kong territory and the Pearl River Delta (PRD) region. Synchronous meteorological and air monitoring data were adopted for analysis with focus on concentration variability, weather pattern, mechanisms of local photochemical production and regional transport. Our results indicate that clear skies with high temperature and low humidity caused by the strong high-pressure system over South China as well as local emissions were attributable to the high O_3 level observed. In addition, backward trajectories and the O_3/NO_x, O_3/CO ratios provided evidence that regional transport did play an important role in the formation of the episode. The MM5/STEM-2K1 and TAPM model systems were used to simulate the regional and urban O_3 pattern in PRD and Hong Kong. The modeling surface concentrations of O_3 were compared with the measurement from Hong Kong air quality monitoring network, which showed that the ground O_3 level was underestimated 10–20% due to the uncertainty in emission data, simple chemical mechanism as well as MM5 meteorological prediction. Sensitivity study revealed the strong cross-border transport over PRD region, which accounted for 50–90% of the observed O_3 level at nighttime and 40–70% at daytime in Hong Kong territory depending on site locations.

1. Introduction

Photochemical smog is formed by a series of complex reactions between nitrogen oxides ($NO_x = NO + NO_2$) and volatile organic compounds (VOCs) in the presence of sunlight and under favorable meteorological conditions. The main constituent of photochemical smog is ozone, which has significant influence on the environment, the ecology as well as the climate. In the past decades, the increase in ozone levels has been one of the most significant atmospheric environmental problems in many mega-cities of China. As a very important city situated in the fast developing Pearl River Delta (PRD) region of South China, Hong Kong has also faced the deterioration of air quality during recent years. Measurements have shown that pollutants such as ozone, nitrogen dioxide, VOCs and particulate matter play important roles in air pollution episodes and cause poor visibility in urban areas. As reported by the HKSAR EPD (HK EPD, 2002), ozone levels in the territory exhibited a slow rising trend since 1991. The annual average of ozone for urban stations in 2002 (27 μgm^{-3}) was 50% higher than the 1991 value (18 μgm^{-3}).

In recent years, air quality studies in Hong Kong and the PRD region, especially for O_3, have received much attention. For example, the intermittent ozone-pollution episodes observed at the site of Cape D'Aguilar at the southeastern tip of the Hong Kong island were reported by Wang et al. (1998). The seasonal, temporal and spatial variation of the surface O_3 at Hong Kong was

*Corresponding author.
e-mail: tjwang@nju.edu.cn
DOI: 10.1111/j.1600-0889.2005.00172.x

analyzed by Chan et al. (1998a,b). As discussed by Chan and Chan (2000), enhanced ozone concentrations were particularly found during summer and autumn. Lam et al. (2001) found that the O_3 maximum in the autumn in Hong Kong was attributed to the long-range transport of high O_3 precursors within the polluted continental air masses as well as the photochemical formation under dry and sunny weather conditions. Wang et al. (2004) used trajectory and regression analysis to investigate the variability and correlation of surface O_3 and CO at the background station of Hong Kong. Ozone episodes during the warm seasons in Hong Kong are usually associated with the passage of tropical storms close to the territory, while the development of pollution episodes in the cool seasons are more related to northeast monsoons with high-pressure systems prevailing over central Asia (Lee et al., 2002). Wang et al. (2003a) reported the chemical characterization of the boundary layer outflow of air pollution to Hong Kong during the Transport and Chemical Evolution over the Pacific (TRACE-P) and ACE-Asia intensive in the spring of 2001. The temporal variability and emission patterns of pollution plumes in the PRD was also investigated by Wang et al. (2003b). Many of these studies involved data analysis of O_3 characteristics based on field measurements. However, there are few studies focusing on the regional distribution of O_3 as well as the mechanisms of chemical transformation and trans-boundary transport in the study region using numerical models.

In this paper, we concentrated on the characteristics of a photochemical pollution episode in Hong Kong during March 27–31, 2000. We first present surface concentrations of O_3, NO_x, CO, RSP and SO_2 recorded at fourteen monitoring stations in Hong Kong and analyze their variability. Then we discuss these results in the context of weather patterns and surface meteorology and their effect on the formation of the pollution episode. The mechanisms of local production and regional transport were discussed. Finally, we used two nested air quality models as well as backward trajectory analysis to simulate the regional and urban surface O_3 patterns and to quantitatively investigate the regional contributions to this episode.

2. Methodology

2.1. Air quality and meteorological data

The hourly air quality data from the monitoring stations of Air Quality Monitoring Network supervised by the Hong Kong Environmental Protection Department were used for this analysis. The pollutants include O_3, CO, NO_x, SO_2 and RSP. Figure 1 shows the locations of the fourteen stations, of which Tap Mun (TM) is a rural station, Central, Mong Kok, Causeway Bay are roadside stations, and others are urban stations.

The weather charts and surface meteorological data were used to analyze the synoptic systems and local characteristics during this episode and to validate the model results over the coastal complex terrain. All these data were provided by the Hong Kong Observatory.

Fig. 1. Locations of the air quality monitoring stations in Hong Kong.

2.2. Air quality models

Two kinds of air quality models, STEM-2K1 and TAPM, focusing on regional and urban scales were used to simulate the flow structure and the O_3 concentration during the episode period. The two models use different meteorology drivers, chemical mechanism and the same emission inventory. STEM-2K1 and TAPM were run separately without connection between the two.

STEM-2K1 is a regional air quality model developed at CGRER (Center of Global and Regional Environmental Research) of the University of Iowa. It employs the SAPRC 99 mechanism (Carter, 2000) that considers 74 species and 211 reactions. Photolysis frequencies are explicitly solved with online tropospheric ultra violent (TUV) model (Tang et al., 2003), including the influences of clouds and aerosols. STEM-2K1 is driven by the mesoscale model MM5. The NCEP $2.5^\circ \times 2.5^\circ$ reanalysis data and monthly averaged sea-surface temperature data were used as initial and boundary conditions. After MM5 was initialized once, then a single forecast was performed for the entire simulation period, just updating the boundary conditions every 6 h from the NCEP re-analysis. The performance of MM5 on meteorological parameters modeling was discussed by Lam et al. (2005). The nesting technique with three resolutions (54 km, 18 km, 6 km) was adopted for both meteorological and chemical models. The STEM-2K1 model performed successfully for the TRACE-P experiment (Carmichael et al., 2003). The emission inventory outside Hong Kong for the model was from Streets et al.'s (2003) work. Biogenic emissions are based on GEIA estimation (Guenther et al., 1995).

The air quality model TAPM (The Air Pollution Model) was also used for our study. It is a nested numerical model focusing on urban and regional scales. The model solves the fundamental fluid dynamics and scalar transport equations to predict meteorology and pollutant concentration for a range of pollutants important for air pollution applications. It consists of

coupled prognostic meteorological and air pollution concentration components, eliminating the need to have site-specific meteorological observations. Instead, the model predicts the flows important to local-scale air pollution, such as sea breezes and terrain induced flows, against a background of larger-scale meteorology provided by synoptic analyses. The 6-h synoptic scale analyses on a longitude/latitude grid at 0.75 grid spacing are used for TAPM. The database is derived from Global Analysis and Prediction (GASP) analysis data from the Australian Bureau of Meteorology (BoM). The chemical mechanism is called Generic Reaction Set (GRS) (Azzi, 1992). TAPM has been used and verified for regions in Australia and other countries (Hurley, 2002). In this work, TAPM was run in three nesting levels (9 km, 3 km, 1 km). The emission inventory outside Hong Kong was also from Streets et al. (2003)'s work. Emission data for Hong Kong area was supplied by HK EPD, 2002.

2.3. The trajectory model

The trajectory model NOAA-HYSPLIT4 (Draxler and Hess, 1997, 1998; Draxler and Rolph, 2003) was applied to calculate backward trajectories to Hong Kong during the episode. The NCEP reanalysis data (ftp://www.arl.noaa.gov/) were used to drive the trajectory model. The spatial resolution is 2.5° × 2.5°. Three-day backward trajectories arriving at 2000 m, 1500 m, 1000 m above sea level were calculated with time step of 1 hr to find out where the air masses came from during the episode.

3. Results and discussions

3.1. Concentration

The ground level concentrations of O_3, NO_x, CO, RSP and SO_2 at the 14 monitoring stations during the episode days were analyzed. Figures 2 and 3 illustrate the hourly and diurnal variations at the four selected stations, which were Tsuen Wan (TW), Central, TM and Tung Chung (TC). These four sites were chosen because they represent residential districts, commercial districts, rural areas and living district in new town, respectively. Therefore, air pollution characteristics in different regions of Hong Kong can be investigated.

3.1.1. Hourly variations. During this period the maximum concentrations of O_3, NO_x, CO, RSP and SO_2 were 265 μgm^{-3}, 2166 μgm^{-3}, 5405 μgm^{-3}, 349.3 μgm^{-3} and 221 μgm^{-3}, respectively. In general, the concentrations of pollutants during March 28 and 29 remained higher than during other days. It is seen that the pollutant concentrations vary significantly at different stations. For TW, the variations of NO_x, RSP, CO and SO_2 concentrations were different from that of O_3. When the concentrations of these four species are high, the O_3 level is low. In addition, the O_3 peak occurs later compared to the other pollutants. These characteristics are also true for other urban stations.

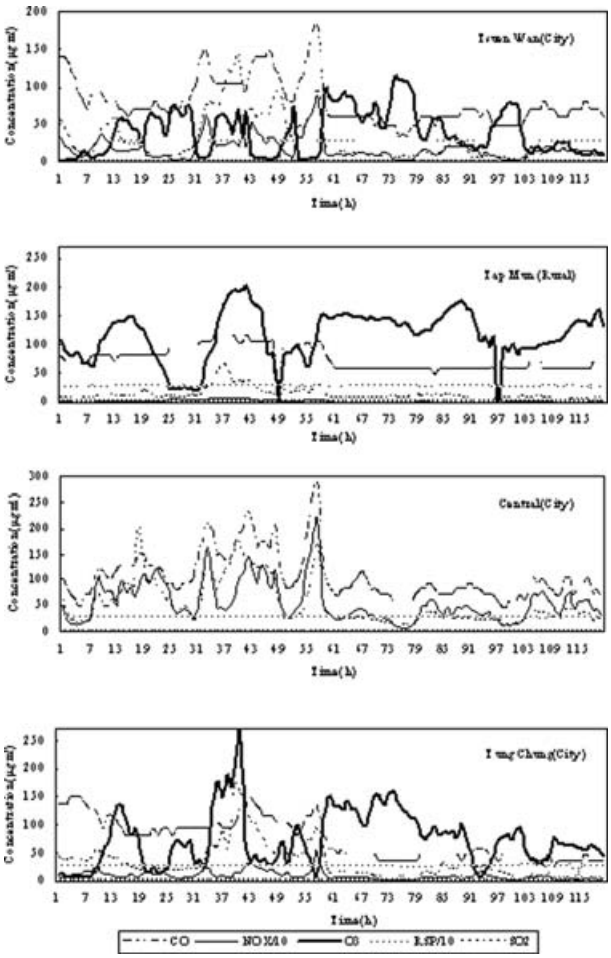

Fig. 2. Hourly concentration variations of the five pollutants from 01:00 March 27 to 24:00 March 31, 2000.

However, for the roadside sites, such as Central station, the pollutant concentrations peak on March 29. The concentrations of NO_x and CO are much higher, while SO_2 concentration is relatively low. A NO_x maximum of 2166 μgm^{-3} was reported at Central during the episode.

In addition, the concentrations of O_3, NO_x, RSP, CO and SO_2 at those stations that are close to the China mainland, such as TC (from west) and TM (from North), are relatively high. For instance, an O_3 maximum of 265 μgm^{-3} was recorded at 17:00 of March 28 at TC, a value exceeding the Hong Kong Air Quality Object for O_3 (240 μgm^{-3}). The average concentration of O_3 at TC during the study period was 112 μgm^{-3}, which is much higher than that at TW (42 μgm^{-3}). For the rural station TM, consistent high concentrations of O_3 (about 150 μgm^{-3}) were observed, especially during the episode days.

3.1.2. Diurnal variations. The diurnal variations of pollutant concentrations exhibited significant difference depending on the site characteristics. At Central, for example, the highest concentrations of RSP, NO_x, CO were 214.9 μgm^{-3}, 227.5 μgm^{-3}, 1571.7 μgm^{-3}, respectively. There are two peaks at about

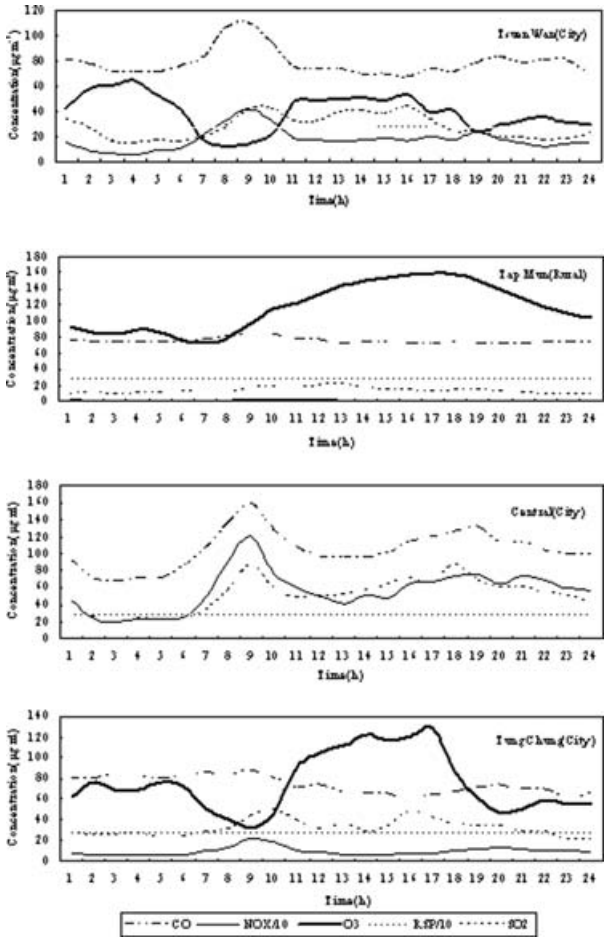

Fig. 3. Diurnal variations of concentrations of the five pollutants.

08:00–09:00 LST and 18:00–19:00 LST, which closely correspond to the traffic rush hours in Hong Kong. The similar diurnal pattern can also be seen at TW, while it is not so strong compared to the roadside station. The NO_x, RSP, CO and SO_2 peaks were observed at 09:00 LST and 21:00 LST. However, O_3 behaves differently. It shows two peaks at 04:00 LST and 15:00 LST. The O_3 peak in the early morning is probably due to the lower inversion height and weak mixing in the urban area compared to the daytime. Also, it may be influenced by the regional transport that will be discussed in Section 3.4.4. The morning ozone peak at TW is of similar magnitude to the other stations, but the afternoon peak is weaker at TW than the other locations, perhaps due to ozone titration from strong NO emissions in the central urban area. In general, the variations of pollutant concentration at the other urban stations are similar to that at TW. The pollutant concentrations at the roadside stations are higher and vary more regularly since they are more influenced by local emissions.

At TM and TC, the diurnal variations of CO, SO_2 and NO_x are not significant compared to TW and Central. The concentration of NO_x was about 20 $\mu gm^{-3}$and 102 μgm^{-3}, which were much lower than 174 μgm^{-3} at TW and 535 μgm^{-3} at Central. In contrast, the O_3 concentration was much higher although the precursor levels were relatively lower. The O_3 levels in suburban areas also showed strong diurnal variations. The O_3 peak appeared at noon and the maximum in the evening disappeared due to the weak mixing in the non-urban area. The averaged concentration of O_3 was 112 μgm^{-3} and 78 μgm^{-3} compared to 42 μgm^{-3} at TW. The characteristics of O_3 diurnal variation at TM and TC suggest that regional transport may play an important role for the concentration variations. However, the local emissions emitted in the city zone around TW may also have influence on O_3 variation at TC due to the prevailing NNE wind on March 28–29.

3.1.3. O_3/NO_x and O_3/CO ratio. The O_3/NO_x and O_3/CO ratio are calculated using the datasets at TM and TW, and the results were illustrated in Fig. 4. As expected, O_3 and NO_x as well as O_3 and CO showed a negative correlation at these urban sites. The O_3/NO_x and O_3/CO ratio were 0.21 and 0.03, respectively, at TW. The correlation coefficient was 0.57 for O_3–NO_x and 0.59 for O_3–CO. The strong correlation and low ratio revealed the typical characteristics of local emission and photochemical production. In contrast, no significant correlation was found between O_3 versus NO_x and O_3 versus CO at the rural sites. High O_3/NO_x (6.29) and O_3/CO (0.1) were found at TM, which are consistent with the measurements at the background station in Hong Kong (Wang et al., 2004), showing that the site was more influenced by regional plumes during the episode days. These differences in O_3/NO_x and O_3/CO ratio and their correlation reflect the chemical characteristics of regional and urban plumes, and this behavior can be used as criteria for tracing the origin of air masses arriving at the sites.

3.2. Meteorology

The surface meteorological factors that are related to this photochemical pollution episode are presented in Table 1. During these episode days (March 28 and 29), the surface wind direction was north–northeast and the wind speed was moderate (2–7 km h^{-1}). These conditions are favorable for air pollutants from the PRD region to be transported to Hong Kong. In addition, air temperatures reached the highest value 27.7°C and relative humidity was the lowest 62%. The weather was generally fine with the sunshine duration hours as long as 9.9 hr. These meteorological conditions of high air temperature and low relative humidity with abundant sunshine are very favorable for the formation of photochemical smog. On March 30 and 31, the surface wind became high (16–20 km h^{-1}), which would dilute the air pollutants and was not beneficial to transport of pollutants from the PRD region.

Figure 5 displayed the surface weather chart on March 28, 2000. It shows that there existed two high-pressure systems in northern and southern China, respectively. Hong Kong was more

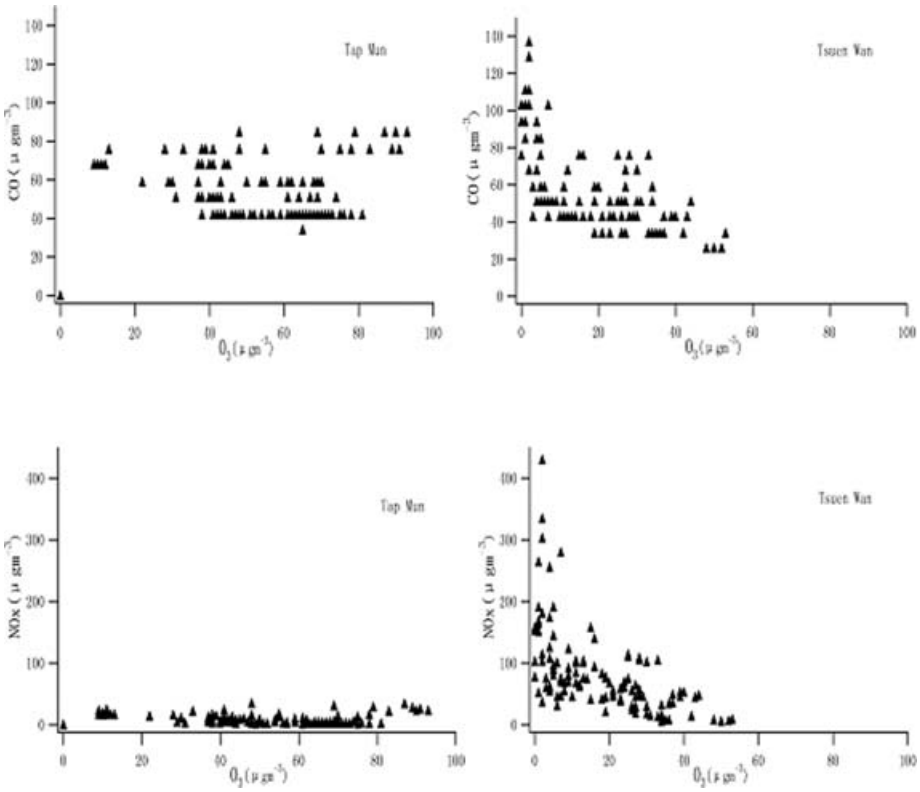

Fig. 4. O_3, CO and NO_x relations at Tap Mun (TM) and Tsuen Wan (TW).

influenced by the high-pressure system over South China. The weather was hot and sunny on that day and the prevailing synoptic winds were from the northeast. On March 29, the high pressure over northern China extended to the south and that over southern China moved to the west. Hong Kong was on the edge of the high-pressure system located in North China and in the front of the high-pressure system located over South China. The weather was almost similar to that of March 28. Hong Kong was on the bottom of the high-pressure system on March 30. The weather was still sunny, however, the dominant synoptic wind arrived at Hong Kong from the east. The high-pressure system moved eastwards the sea on March 31.

As indicated above, on March 28 and 29, 2000, Hong Kong was basically under the control of a high-pressure system. The air temperature was high and relative humidity was low. There were almost no clouds. Thus, solar radiation was intense and sunshine hours were long, which were all favorable for the formation of photochemical smog. Because of lying on the front edge of the high-pressure system on these 2 d, the dominant synoptic wind influencing Hong Kong came from the northeast. Therefore, air pollutants could easily be transported from mainland China, especially the PRD region, to Hong Kong territory.

3.3. Mechanisms

3.3.1. Local effect. There are a few key factors that can affect the formation of photochemical pollution: high level of precursors, such as hydrocarbons and NO_x; intensive sunshine;

Table 1. Ground level meteorological data during March 27–31, 2000.

Time	Wind speed (km h^{-1})	Wind direction	Maximum air temperature (°C)	Relative humidity (%)	Sunshine duration (hr)	Weather
March 27	12	NNE	22.4	76	2.1	Cloudy
March 28	2	NE	23.9	81	7.9	Sunny
March 29	7	NNE	27.7	62	9.9	Sunny
March 30	16	NNE	25.3	63	9.9	Sunny
March 31	20	NE	24.6	87	6.7	Sunny

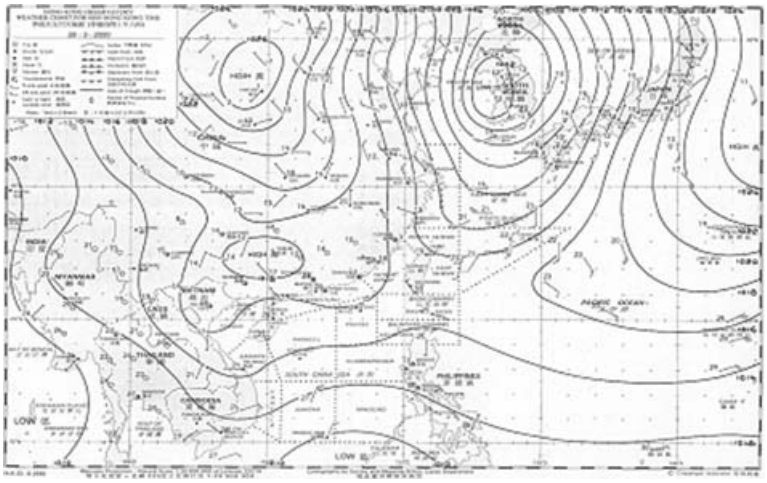

Fig. 5. Surface weather chart on 08:00 LST March 28, 2000.

complex terrain and condensed buildings that can accumulate air pollutants. Hong Kong is a metropolis with heavy traffic. The NO_x levels in the air are high. In addition, hilly areas make up about 70% of Hong Kong, and there are many tall buildings in the urban area, so the pollutant cannot diffuse with ease. Furthermore, the weather during these days was beneficial to initiate and to promote photochemical reactions. Therefore, episodes of photochemical pollution can easily occur in Hong Kong. The strength of the photochemical smog can be measured by O_3 that is the main product of photochemical reactions. During the study period, the concentration of O_3 was very high with a maximum of 265 μgm^{-3} observed in west Hong Kong. This value exceeded the Hong Kong Air Quality Objective (240 μgm^{-3}).

In urban areas of Hong Kong, such as TW and the Central stations, the highest concentrations of NO_x, CO and RSP are usually found during the traffic rush hours, 09:00 LST and 21:00 LST. Vehicles exhaust gases that mainly consist of these pollutants, and air quality in urban Hong Kong can be heavily impacted by the local vehicular emissions. When human activities start in the morning (ca. 07:00–10:00 LST), NO_x levels gradually increase. Since solar radiation is still weak, O_3 decreases and reaches a minimum due to the reaction between O_3 and NO. With the enhancement of sunlight and vertical mixing in the daytime, the level of O_3 gradually increases, and reaches its peak ca. 13:00 LST. At the same time, the NO_x level decreases. As far as the O_3 peak at 04:00 LST is concerned, it is caused by the more stable atmospheric condition, which prevents strong diffusion of O_3. Additionally, low concentrations of NO at night cannot destroy O_3 efficiently. This suggests that local photochemical reactions drive the diurnal cycle of this pollution episode at the urban sites.

3.3.2. Regional effect. Apart from the local influence, regional effects on air pollutant concentration should not be ignored at most sites. At TM station there is no heavy traffic. The level of NO_x is low, however, the concentration of O_3 is higher compared to the urban sites. It is possible that the impact of local emissions is not important in these rural areas. Instead, regional transport from the China mainland may play a critical role as the concentrations of O_3 and SO_2 at the sites close to the PRD region are relatively higher than those at the other sites. On the other hand, NO_x at TC is not very low, suggesting that O_3 and SO_2 at TC can also be affected by the emissions from TW under favorable wind. Here, we analyzed the daily averaged concentration variations of O_3 and SO_2 at TM, TC, Yuen Long (YL), Tai Po (TP), Sha Tin (ST), TW, Kwai Chung (KC) and Sham Shui Po (SSP), and linked them to the regional surface winds in the PRD region as well as the local surface winds in Hong Kong.

Figure 6 shows the daily average O_3 concentrations at the eight representative stations during March 28–31, 2000. On March 28, the concentrations of O_3 at all sites, except for TM, are very low. The O_3 level at each site increase on March 29. But on the next 2 d, it has a decreasing trend. This behavior can be understood by taking the surface winds into account. During the episode days, the prevailing synoptic winds over PRD were north or northeasterly, and O_3 from the PRD region could be transported to Hong Kong and, thereby causing the high O_3 concentration. However, when the winds changed to easterly, the O_3 levels at every station gradually fell, as a result of the mixing of the clean air from the sea.

The variations of SO_2 concentrations at the eight sites during this episode are shown in Fig. 7. When the prevailing synoptic winds are north or northeasterly (March 28–29), the concentration of SO_2 at each site is very high. With the changing of wind direction, it sharply decreased. Since there are almost no large and heavily polluted industries in Hong Kong, local emissions of SO_2 are expected to be very small. Hence, variations of SO_2 concentrations from March 27 to 30 at the eight stations signify the role of regional transportation in this episode.

In summary, during the episode days, the dominant wind arriving in Hong Kong is from north or northeast, which can result in the transport of pollutants from the upwind region (mainland) to the downwind region (Hong Kong). These results also show that regional transport plays a crucial role on the observed high concentrations of O_3 and other pollutants in this episode.

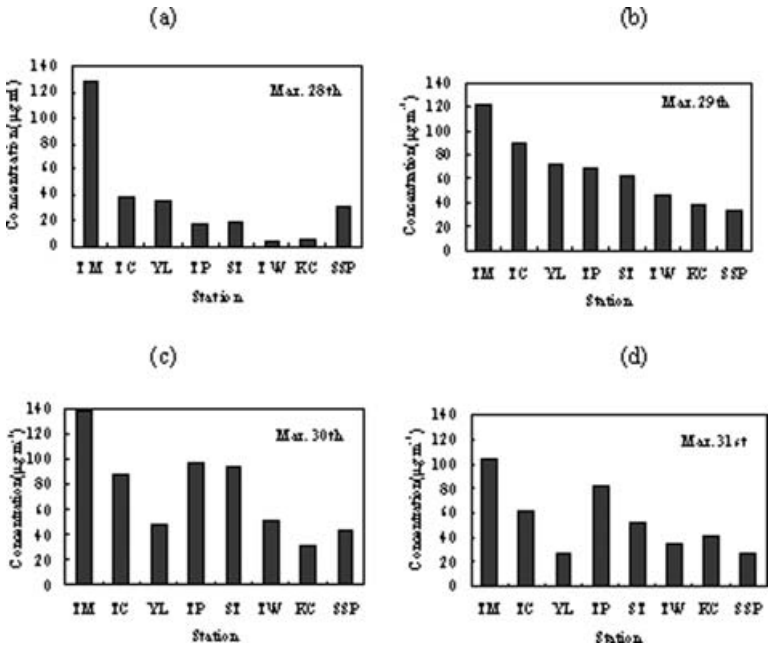

Fig. 6. Daily average O_3 concentrations at eight representative sites.

3.4. Modeling results

To investigate the spatial distribution of flow structure and O_3 concentration in the study region in more detail, two nested air quality models STEM-2K1 and TAPM were run separately for 5 d from March 27 to 31, 2000. The results are discussed below.

3.4.1. Flow structure. Figures 8(a)–8(d) shows the low-level flow pattern over the East-South China, South China, the PRD region and the Hong Kong territory for the simulation period. In the afternoon of March 28, strong outflow was simulated over the continent of China. North and northeasterly winds were prevailing in the study region due to the influence of high-pressure system, which developed over the north of mainland China. However, at the surface, the wind over Hong Kong is more irregular due to its complex terrain and land-sea distribution. Northeasterly winds were dominant over the main parts of territory. The east of Hong Kong is controlled by northeast winds. In southern Hong Kong, the winds were from the west. Under the control of the high-pressure system, the weather in Hong Kong is hot

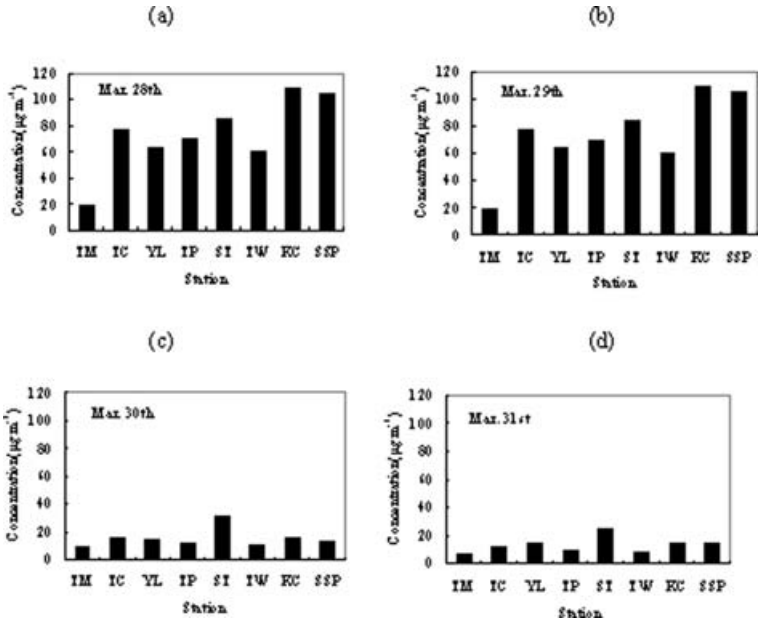

Fig. 7. Daily average SO_2 concentrations at eight representative sites.

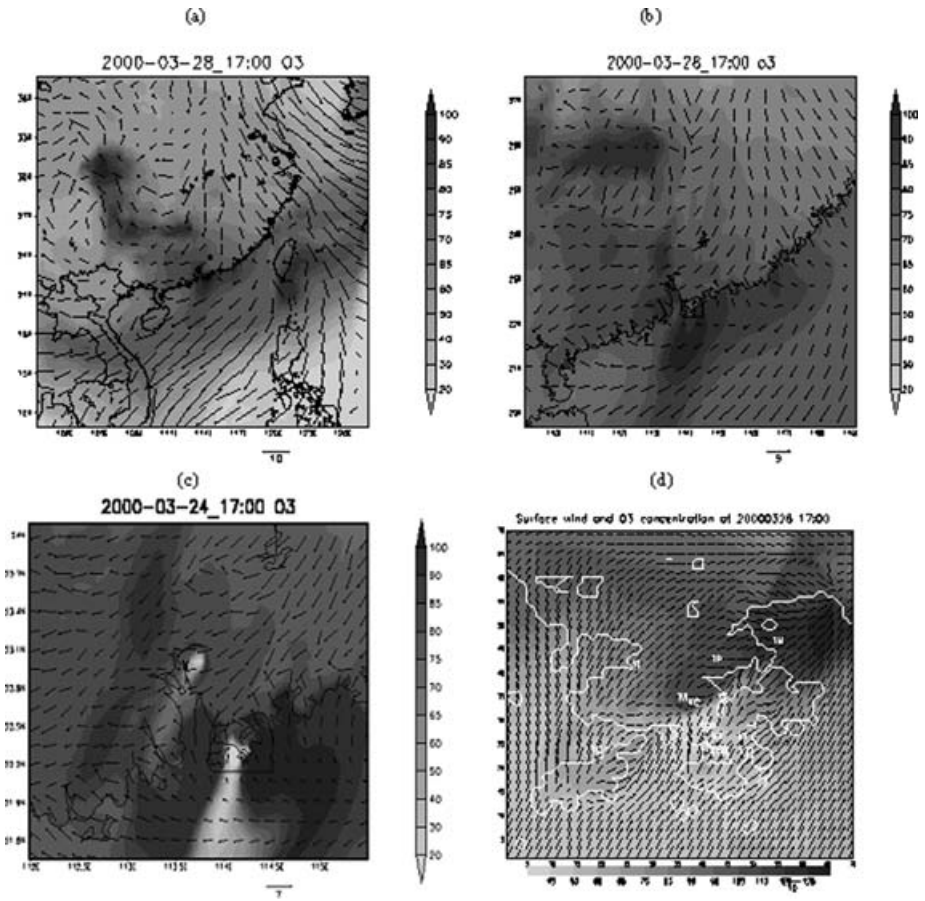

Fig. 8. Modeling surface wind and O_3 at March 28, 2000, 17:00 LST over Hong Kong and PRD region with different resolution (a) 54 km level, (b) 18 km, (c) 6 km and (d) 1 km.

and sunny, which is beneficial to the formation of ozone. Also, the dominant northeasterly winds brought regional ozone and its precursors from the continent, which had a great impact on the ozone pattern in Hong Kong.

3.4.2. Surface ozone. The predicted surface ozone during the episode is also illustrated in Fig. 8. Here, the modeling results from 54 km, 18 km and 6 km resolutions of STEM-2K1 run and 1 km resolution of TAPM run are presented. Due to horizontal advection caused by the dominant northeasterly winds, the ozone plume was transported from the PRD region to the Hong Kong area. Noticeably, the surface ozone concentration is enhanced dramatically over the territory on March 28, 17:00 LST. The simulated surface ozone from 1 km resolution was compared with the measurements at several stations in Fig. 9. The modeling of ozone concentrations exhibited a general agreement with observations. Moderate positive correlations between the observed and predicted O_3 was found at several sites. The observed ozone peaks were captured, however, they were underestimated by 10–20% compared to the measurement. At TC station, the observed O_3 level larger than 200 μgm^{-3} are not well reproduced. The difference between the predicted and observed peak concentrations were partly attributable to the uncertainty in NO_x and VOC emission data over the study region. Therefore, emission inventory with higher resolution and accuracy are expected to improve the model results. On the other hand, the semi-empirical chemical mechanism of GRS used in TAPM may also contribute to this underestimation. In addition, the error in MM5 prediction can also affect the modeling results.

3.4.3. Backward trajectories. To investigate the signature of cross-border transport of air pollutants over PRD on the regional scale, backward trajectories were applied to examine the typical air masses arriving at Hong Kong during the episode period. Three-day backward trajectories to Hong Kong at different levels (1000 m, 1500 m, 2000 m) in the boundary layer were calculated using NCEP reanalysis data as shown in Fig. 10. On the episode day the trajectories came from the northwest and then turned to south and passed through South China as well as the PRD region before reaching Hong Kong. The northerly winds in the boundary layer induced by the continental high-pressure system were beneficial to cross-border transport of ozone and its precursors to the Hong Kong area. On March 31, the high pressure moved eastwards to the ocean, the wind direction changed from north

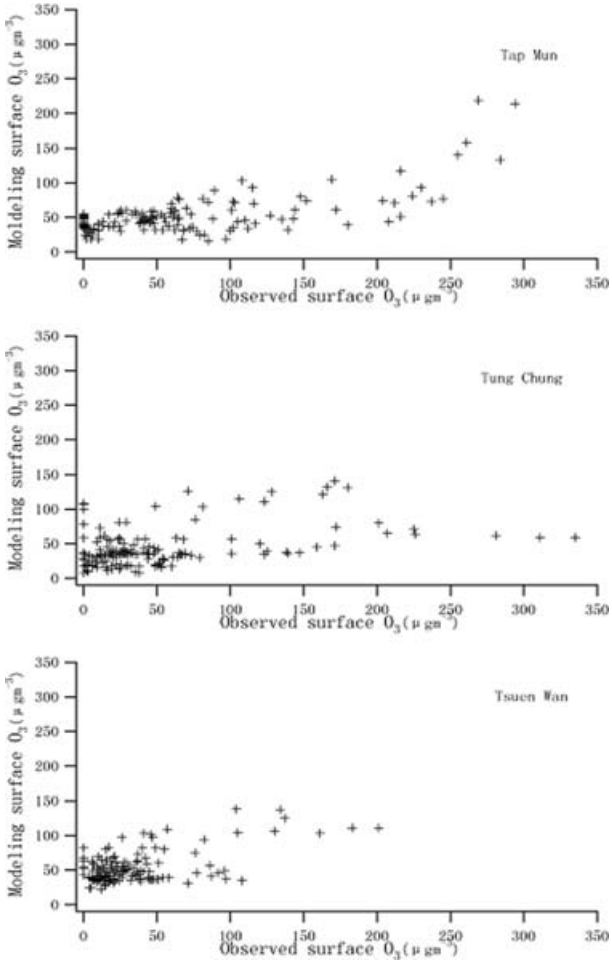

Fig. 9. Modeling surface O_3 at selected sites of Hong Kong.

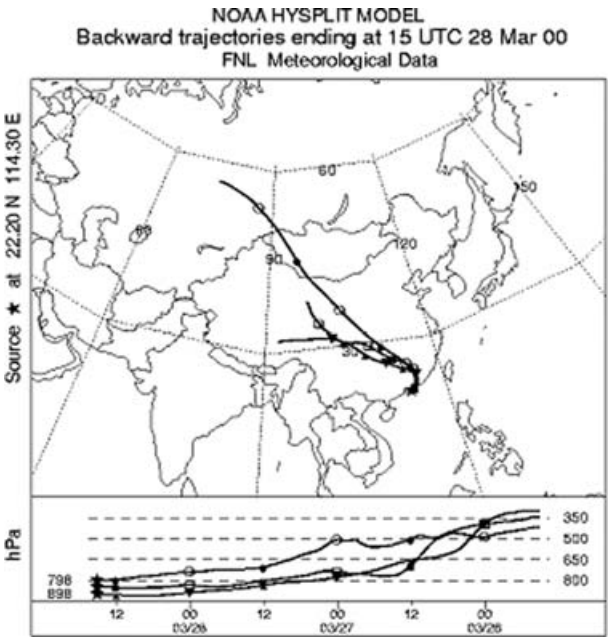

Fig. 10. Seventy-two hours backward trajectories to Hong Kong at 2000 m, 1500 m and 1000 m on March 28, 2000.

to east and much cleaner air masses from the Pacific diluted the high ozone concentration, and the episode came to an end. The backward trajectory analysis further supports the possible transport of air pollutants from PRD due to the continental outflow, and subsequent influence on air quality in Hong Kong.

3.4.4. Regional contribution. To further quantitatively understand the regional transport from the PRD on the Hong Kong air quality, the emissions inside the Hong Kong area were set to zero and TAPM was run again for the same period as the base case. The ratio of predicted surface ozone when only Hong Kong external emissions were considered to that when all emissions were considered was calculated. Thus, we can apportion the percentage of air pollution from cross-border transport from the PRD region against that from Hong Kong itself. Figure 11 illustrates the temporal ratio at the four stations during the two episode days. The ratios show strong diurnal variation with low values in the daytime and high values at night. This reveals that regional transport is more important during the nighttime because of favorable winds for transport and no chemical production of ozone. However, the regional effects vary depending on time and location of the sites. Generally, regional transport contributes 50–90% at night and 40–70% during daytime. It should be noticed that the non-linearity of ozone chemistry might have an effect on the model results to certain extent, which need to be further investigated. Anyway, the results from this sensitivity study are consistent with those from the trajectory analysis, further confirming the importance of cross-border transport for this high ozone event.

4. Conclusions

The air pollution episode, occurring in Hong Kong during March 27–31, 2000, was a typical case with characteristics of photochemical smog. Both local production and regional transport

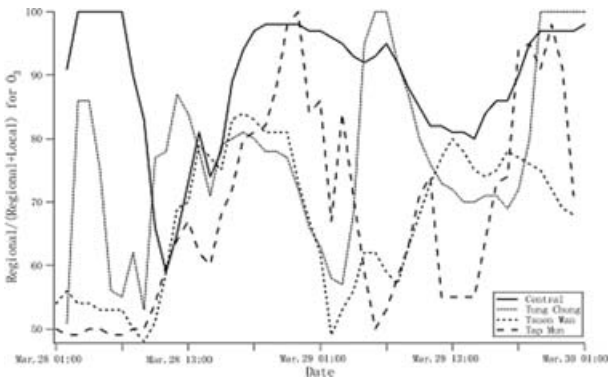

Fig. 11. Percentage of regional effect on surface ozone at monitoring sites.

contributed to this episode. The episode lasted 2 d in Hong Kong area, where the high concentrations of O_3, NO_x, CO, RSP and SO_2 of 265 μgm^{-3}, 2166 μgm^{-3}, 5405 μgm^{-3}, 349.3 μgm^{-3} and 221 μgm^{-3} were recorded.

The synchronous meteorological data and air monitoring data were adopted for the analysis with focuses on concentration variation, weather pattern, the mechanisms of local photochemical production and regional transport. Investigations showed that diurnal variations of O_3 and other pollutants were significant at urban sites because of strong local emissions. However, due to the influence of regional transport, non-urban sites exhibited weak diurnal variations. During the episode days, the Hong Kong territory was under the control of the continental high-pressure system. The hot and sunny weather as well as anthropogenic emissions were beneficial to the formation of photochemical smog. The prevailing synoptic wind in Hong Kong was from the northeast. Trajectory analysis and sensitivity study suggested that high levels of O_3 and other pollutants in Hong Kong could be caused by regional transport from the upwind PRD area. It was estimated that the influence of regional transport could contribute 50–90% of surface O_3 at nighttime and 40–70% at daytime.

5. Acknowledgments

This work was founded by START Fellowship Award, the Hong Kong Polytechnic University (ASD project A514) and the National Key Basic Research Support Foundation of China (2002CB410811). The authors would like to thank the Hong Kong Environmental Protection Department for providing emission inventory and air quality monitoring data and the Hong Kong Observatory for providing meteorological data. The authors gratefully acknowledge the NOAA Air Resources Laboratory (ARL) for providing of the HYSPLIT transport and dispersion model (http://www.arl.noaa.gov/ready.html) used in this publication.

References

Azzi, M., Johnson, G. M. and Cope, M. 1992. An introduction to the generic reaction set photochemical smog mechanism. Proceedings of the 11th International Clean Air and Environment Conference, Brisbane, 1992, Clean Air Society of Australia & New Zealand.

Carmichael, G. R. Y., Tang, G., Kurata, I., Uno, D. G., Streets, J.-H. and co-authors. 2003. Regional-scale chemical transport modeling in support of intensive field experiments: overview and analysis of the TRACE-P Observations. *J. Geophys. Res.* **108**(D21), 8823–8849.

Carter, W., 2000. Documentation of the SAPRC-99 chemical mechanism for voc reactivity assessment, Final Report to California Air Resources Board Contract No. 92–329, University of California-Riverside, May 8, 2000. Available at http://www.cert.ucr.edu/∼carter/bycarter.htm.

Chan, L. Y., Liu, H. Y. and Lam, K. S., 1998a. Analysis of the seasonal behavior of tropospheric ozone at Hong Kong. *Atmos. Environ.* **32**(2), 159–168.

Chan, L. Y., Chan, C. Y. and Qin, Y. 1998b. Surface ozone pattern in Hong Kong. *J. Appl. Meteorol.* **37**(10), 1153–1165.

Chan, C. Y. and Chan, L. Y. 2000. Effect of meteorology and air pollutant transport ozone episodes at a subtropical Asian city, Hong Kong. *J. Geophys. Res.* **105**(D16), 20 707–20 724.

Draxler, R. R. and Hess, G. D. 1997. *Description of the Hysplit_4 Modeling System*. NOAA Technical Memorandum; ERL ARL-224; Silver Spring, Maryland, December 1997.

Draxler, R. R. and Hess, G. D., 1998. An overview of the Hysplit_4 modeling system for trajectories, dispersion and deposition. *Aust. Meteorol. Mag.* **47**, 295–308.

Draxler, R. R. and Rolph, G. D. 2003. *HYSPLIT (HYbrid Single-Particle Lagrangian Integrated Trajectory) Model access via NOAA ARL READY* Website (http://www.arl.noaa.gov/ready/hysplit4.html). NOAA Air Resources Laboratory, Silver Spring, Maryland.

Environmental Protection Department, HKSAR. 2002. Report on Study of Air Quality in Pearl River Delta Region. Available at http://www.epd.gov.hk.

Guenther, A., Hewitt, C. N., Erickson, D., Fall, R., Geron, C. and co-authors. 1995. A global-model of natural volatile organic-compound emissions. *J. Geophys. Res.* **100**(D5), 8873–8892.

Hurley, P. 2002. The Air Pollution Model (TAPM) Version 2. Part 1: technical description. CSIRO Atmospheric Research Technical Paper No. 55. Available at http://www.dar.csiro.au.

Lam, K. S., Wang, T. J., Chan, L. Y., Wang, T. and Harris, J. M. 2001. Flow patterns influencing the seasonal behavior of surface ozone and carbon monoxide at a coastal site near Hong Kong. *Atmos. Environ.* **35**(18), 3121–3135.

Lam, K. S., Wang, T. J., Wu, C. L. and Li, Y. S. 2005. Study on an ozone episode in hot season in Hong Kong and transboundary air pollution over Pearl River Delta region of China. *Atmos. Environ.* **39**, 6737–6750.

Lee, Y. C., Calori, G., Hills, P. and Carmichael, G. R. 2002. Ozone episodes in urban Hong Kong 1994–1999. *Atmos. Environ.* **36**, 1957–1968.

Streets, D. G., Bond, T. C., Carmichael, G. R., Fernandes, S. D., Fu, Q. and co-authors. 2003. An inventory of gaseous and primary aerosol emissions in Asia in the year 2000. *J. Geophys. Res.* **108**(D21), 8809–8832.

Tang, Y., Carmichael, G. R., Uno, I., Woo, J.-H., Kurata, G. and co-authors. 2003. Impacts of aerosols and clouds on photolysis frequencies and photochemistry during TRACE-P, part II: three-dimensional study using a regional chemical transport model. *J. Geophys. Res.* **108**(D21), 8822–8837.

Wang, T., Lam, K. S., Lee, A. S. Y., Pang, S. W. and Tsui, W. S.1998. Meteorological and chemical characteristics of the photochemical ozone episodes observed at Cape D'Aguilar in Hong Kong. *J. Appl. Meteorol.* **37**, 1167–1177.

Wang, T., Ding, A. J., Blake, D. R., Zahorowski, W., Poon C. N., and Li, Y. S. 2003a. Chemical characterization of the boundary layer outflow of air pollution to Hong Kong during February–April 2001. *J. Geophys. Res.* **108**(D20), 8787–8802.

Wang, T., Poon, C. N., KwokY. H., and Li, Y. S. 2003b. Characterizing the temporal variability and emission patterns of pollution plumes in the Pearl River Delta of China. *Atmos. Environ.* **37**, 3539–3550.

Wang, T. J., Lam, K. S., Tsang, C. W., and Kot, S. C. 2004. On the variability and correlation of surface ozone and carbon monoxide observed in Hong Kong using trajectory and regression analyses. *Adv. Atmos. Sci.* **21**(1), 141–152.